



QUANTUM COMPUTATIONAL ANALYSIS OF ETHYL 6-(CHLOROMETHYL)-4-(4-CHLOROPHENYL)-2-OXO-1,2,3,4-TETRAHYDROPYRIMIDINE-5-CARBOXYLATE USING SPECTRAL METHODS

Shakila G^{1*}, Saleem H², Bharanidharan S³ and Suresh M⁴

¹Department of Physics, Bharathidasan Government College for Women, Puducherry-605003, India

²Department of Physics, Annamalai University, Annamalainagar-608002, Tamilnadu, India

³Department of Physics, Bharath Institute of Higher Education and Research, Bharath University, Chennai-600 073, Tamilnadu, India

⁴Department of Chemistry, College of Engineering, Anna University, Chennai-620025, Tamilnadu, India

ARTICLE INFO

Article History:

Received 16th November, 2017

Received in revised form 13th

December, 2017

Accepted 3rd January, 2018

Published online 28th February, 2018

Key words:

ECM4CTC, FT-IR, FT-Raman, UV-Vis analysis, TED, NBO, NLO.

ABSTRACT

The spectral cum computational analysis of Ethyl 6-(chloromethyl)-4-(4-chlorophenyl)-2-oxo-1,2,3,4-tetrahydropyrimidine-5-carboxylate (**ECM4CTC**) was carried out by using FT-IR, FT-Raman and UV-Vis spectroscopic techniques. The optimization of the structure was performed using DFT/B3LYP/6-311++G(d,p) level. The optimized structural parameters such as bond lengths and bond angles of ECM4CTC were compared with XRD data of the molecule. The Nonlinear optical (NLO) property of the molecule was predicted using computation of first order hyperpolarizability value. Stability of the molecule arising from hyper conjugative interactions, charge delocalization have been analyzed using natural bond orbital (NBO) analysis. The chemical hardness and softness were calculated from the HOMO and LUMO values. MEP surface shows the electrophilic and nucleophilic attack region of the molecule. The Mulliken atomic charges in the molecule were also calculated using the same basis set Mulliken atomic charge (MAC) method.

Copyright©2018 **Shakila G et al.** This is an open access article distributed under the Creative Commons Attribution License, which permits unrestricted use, distribution, and reproduction in any medium, provided the original work is properly cited.

INTRODUCTION

In recent years, pyrimidines containing the bridge head nitrogen atom and their dihydro derivatives, among which promising biologically active compounds were found [Fedorova *et al.*, 2003]. Pyrimidines and their derivatives are considered to be important for drugs and agricultural chemicals. They are also found to exhibit remarkable pharmacological activities such as anti-cancer, anti-tumor, anti-inflammatory and anti-fungal etc and are used widely as agrochemicals, pharmaceuticals, dyes, organic additives in electroplating of steel and in the polymerization process [Sharma *et al.*, 2014 and Vaisalini *et al.*, 2012]. Dihydropyrimidinones, the product of the Biginelli reaction, are also widely used in the pharmaceutical industry [Beena *et al.*, 2012]. Phenyl and its derivatives are biologically and industrially useful compounds, widely used in the manufacturing of dyes, drugs, plastics, explosives, and pesticides, etc. Chlorophenyl is another industrial chemical which got a variety of uses ranging from preparation of preservatives to insecticides.

The inclusion of halogen (chlorine) in phenyl leads to the variation of charge distribution in molecules and consequently affects the structural, electronic and vibrational properties. Generally, chloro group is referred to as electron withdrawing substituent in aromatic systems [Bist *et al.*, 1967 and Evans, 1960].

The literature survey indicates that the quantum chemical analysis with the support of spectral data have not been reported on ECM4CTC so far. Therefore, the present investigation was undertaken to study the structural, non-linear optical, vibrational, electronic, transitional and thermal properties of the molecule, using quantum computational B3LYP method and 6-311++G(d,p) basis set.

Computational Details

The DFT has been proven to be extremely useful in treating electronic structure of molecules. The entire calculations in this study were performed at B3LYP/6-311++G(d,p) level of functional and basis set using Gaussian 03W [Frisch *et al.*, 2004] software on a Pentium IV/3.02GHz personal computer, invoking gradient geometry optimization [Frisch *et al.*, 2004 and Schlegel, 1982]. To investigate the reactive sites of the title compound, the molecular electrostatic potential (MEP)

*Corresponding author: **Shakila G**

Department of Physics, Bharathidasan Government College for Women, Puducherry-605003, India

surface scan analysis was performed. The Total energy distribution (TED) values are computed for every vibrational modes using VEDA4 program [Jamroz, 2004]. The Raman activities were transformed into Raman intensities using *Raint* program [Michalska, 2003 and Michalska *et al.*, 2005]. The wave numbers and geometrical parameters were computed using B3LYP methods with 6-311++G(d,p) basis set. The geometry corresponding to the real minimum on the potential energy surface (PES) has been obtained and the UV-Visible spectra electronic transition such as HOMO-LUMO excitation energies and oscillator strength were calculated using time-dependent TD-SCF-B3LYP method. The NBO calculations were carried out using NBO 3.1 program. In addition, Mullikan charges, dipole moment, the linear polarizability and first-order hyper polarizability of the title molecule are also computed using B3LYP method with same basis set.

Experimental Details

Synthesis Procedure

The compound under investigation was synthesized by heating a mixture of ethyl-4-chloro acetoacetate (4.1 ml, 0.025 mol), 4-chlorobenzaldehyde (3.6 g, 0.025 mol), and urea (4.5 g, 0.075 mol) in ethanol (5 ml) under reflux in the presence of concentrated HCl (1 mL) for 5 h (monitored by TLC). The reaction mixture, after being cooled to room temperature, was poured onto crushed ice and stirred for 5–10min. The solid was separated and filtered under suction, washed with ice-cold water (50 ml), and then recrystallized from hot ethanol to afford pure product [m.p. 437 K; yield 76%]. The structure of the title molecule is shown below in Fig 1a.

Spectral details

The FT-IR spectrum of the synthesized ECM4CTC was recorded in the range 4000–400 cm^{-1} with a spectral resolution of 4 cm^{-1} on SHIMADZU FT-IR affinity Spectrophotometer by KBr pellet technique in the department of Marine Biology, Annamalai University, Parangipettai. The FT-Raman spectrum was recorded on BRUKER: RFS27 spectrometer operating at laser 100 mW in the spectral range of 4000–50 cm^{-1} . FT-Raman spectral measurements were carried out from Sophisticated Analytical Instrument Facility (SAIF), Indian Institute of Technology (IIT), Chennai. The UV-Vis absorption spectrum of ECM4CTC was recorded in the range of 200–500 nm using a Shimadzu-2600 spectrometer in the department of Chemistry, Jamal Mohamed College, Tiruchirappalli, Tamilnadu.

RESULTS AND DISCUSSION

Geometrical Analysis

The quantum chemical calculations were utilized to find the optimized structure of the ECM4CTC using B3LYP/6-311++G(d,p) level of theory. Since dispersion energies do not play a considerable role in these types of structure, electron correlations are not so important consequently DFT methods would provide a good quality structures. The single crystal X-ray structure for the novel ethyl 6-(chloromethyl)-4-(4-chlorophenyl)-2-oxo-1,2,3,4-tetrahydro pyrimidine-5-carboxylate molecule was reported [Bharanidharan *et al.*, 2014]. The optimization process goes smoothly till reached a local minimum after 47 steps as shown in Figs. 1b and 1c, respectively. Fig. 1a shows the optimized structure of

ECM4CTC molecule showing the atom symbols and numbering scheme, respectively.

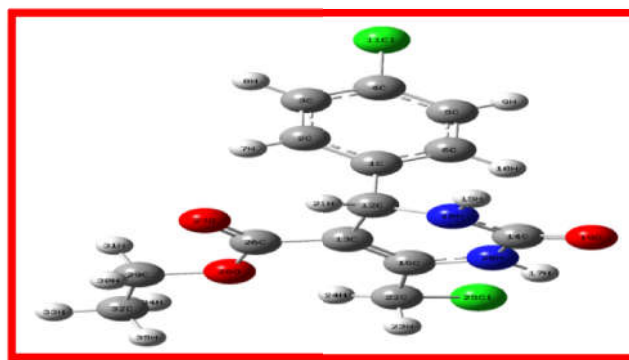


Fig 1a Optimized structure of ECM4CTC

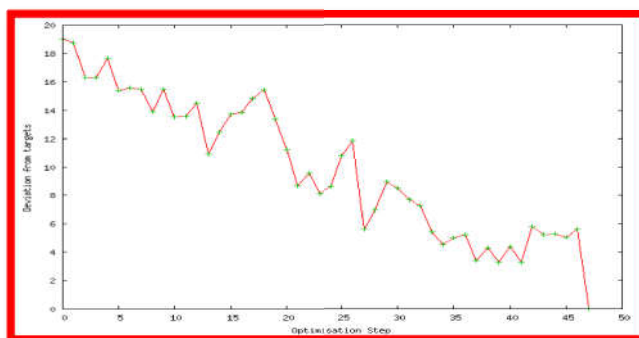


Fig. 1c. Optimization steps vs Energy of ECM4CTC

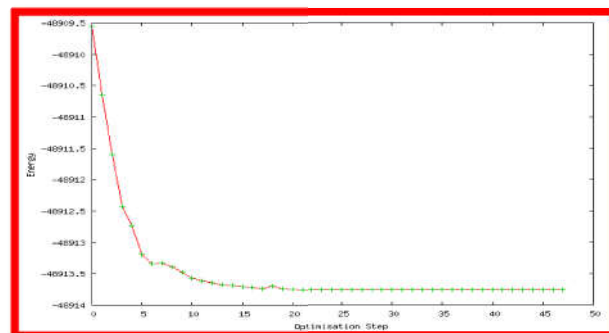


Fig 2 Frontier molecular orbital diagram of ECM4CTC

The selected bond parameters such as bond lengths, bond angles and dihedral angles values are presented in Table. 1 and also compared with reported XRD data.

Table 1 The selected bond parameters of ECM4CTC

Bond Parameters	B3LYP/6-311++G(d,p)	XRD ^a
Bond Lengths (Å)		
C12-C13	1.531	1.513 (2)
C12-N18	1.464	1.461 (2)
C13-C16	1.363	1.341 (3)
C13-C26	1.474	1.466 (3)
C14-N18	1.365	1.333 (3)
C14-O19	1.221	1.225 (2)
C16-N20	1.380	1.379 (2)
C22-C125	1.825	1.766 (2)
C26-O27	1.222	1.207 (3)
C26-O28	1.356	1.330 (3)
C29-O28	1.450	1.482 (8)
C29-C32	1.516	1.430 (19)
Bond Angles (°)		
C12-C13-C16	118.583	119.80 (17)
C12-C13-C26	113.488	117.78 (17)
C16-C13-C26	127.914	122.35 (17)
N18-C14-O19	125.322	123.56 (18)

N18-C14-N20	113.398	115.73 (17)
O19-C14-N20	121.249	120.66 (19)
C13-C16-N20	119.377	120.01 (17)
C13-C16-C22	126.251	124.57 (18)
N20-C16-C22	114.242	115.41 (18)
C12-N18-C14	124.034	124.46 (16)
C14-N20-C16	125.098	123.10 (17)
C16-C22-C125	112.223	112.02 (15)
C13-C26-O27	122.586	127.3 (2)
C13-C26-O28	115.791	110.28 (17)
O27-C26-O28	121.614	122.43 (19)
C26-O28-C29	115.605	114.8 (8)
O28-C29-C32	107.561	107.3 (12)
Dihedral Angles (°)		
C12-C13-C26-O28	179.3034	-173.0 (2)
C16-C13-C26-O27	176.7652	-168.2 (2)
C26-O28-C29-C32	179.5562	171.9 (10)
O28-C29-C32-H33	179.6579	177.8 (9)

^oCrystal structure of ethyl 6-(chloromethyl)-4-(4-chlorophenyl)-2-oxo-1,2,3,4-tetrahydropyrimidine-5-carboxylate S. Bharanidharan, H. Saleem, B. Gunasekaran, M. Syed Ali Padusha and M. Suresh

The CC bond length values inside the phenyl ring lies in the range 1.401 Å to 1.394 Å, the corresponding XRD values are 1.342 Å to 1.388 Å, respectively. But the pyrimidine ring CC values lies in the range 1.363 Å to 1.531 Å. This difference in values indicate the conjugational difference between the pyrimidine and phenyl ring, which shows the electronic distribution inside these two rings are slightly different. The single bonded C-C has the bond length values in the range 1.45 to 1.50 Å, while the double bonded CC values in the range 1.33 to 1.34 Å. The table shows C₁₂-C₁₃ bond length is 1.531 Å and that of C₁₃-C₂₆ is 1.474 Å, which indicates they are purely single bonded but with a different electronic density or distribution. According to the bond length values computed for this molecule, there is no CC bond which is purely double bonded but some of the bonds in the phenyl and pyrimidine rings are closer to double bonded CC, which can be identified through vibrational analysis.

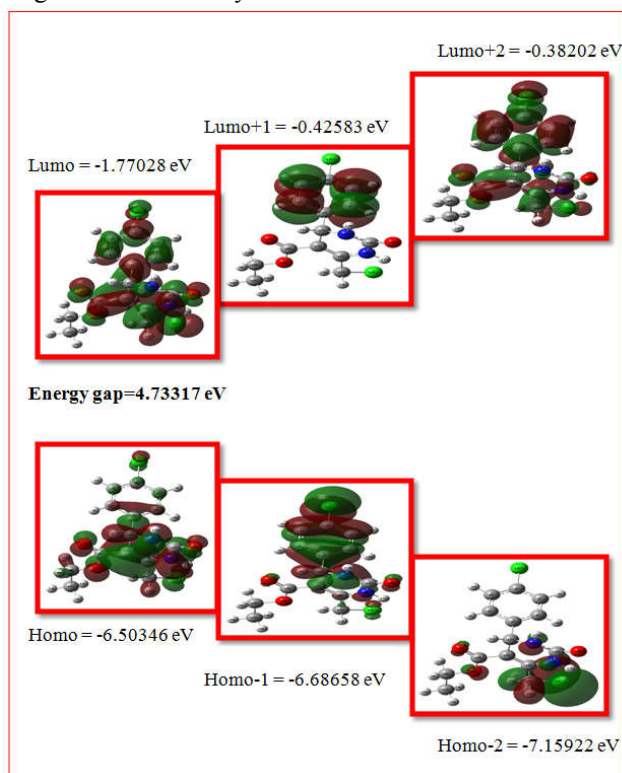


Fig 2 Frontier molecular orbital diagram of ECM4CTC

The average bond distances of C₁₄-N₁₈ and C₁₆-N₂₀ in the pyrimidine ring calculated by DFT method are 1.366 Å and 1.380 Å, respectively

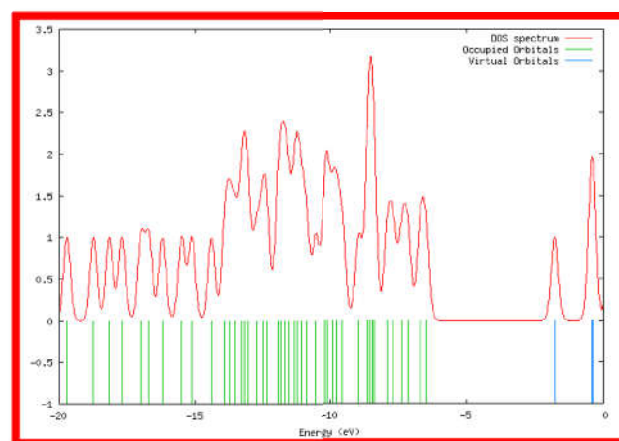


Fig 3 DOS spectrum of ECM4CTC

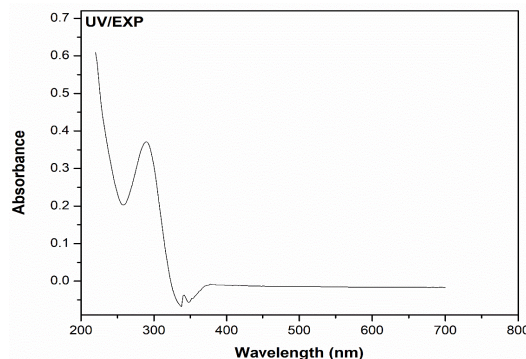
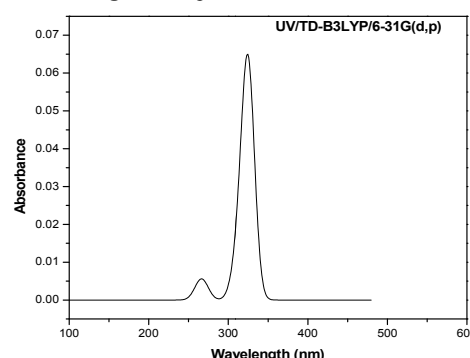


Fig 4 The combined theoretical and experimental UV-Vis spectra of ECM4CTC

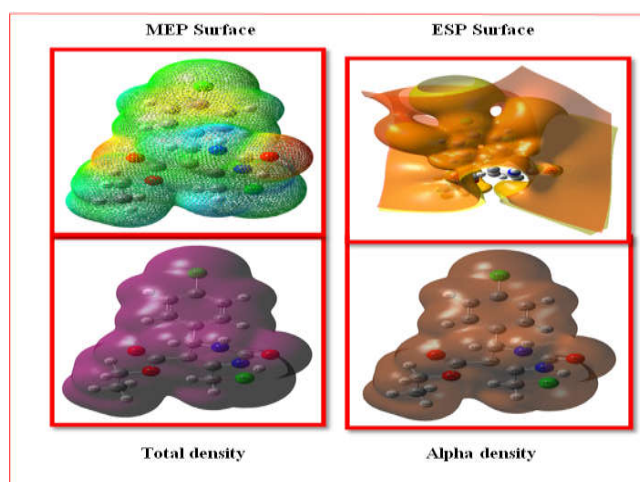


Fig 5 The Total density, Alpha density and MEP Surfaces of ECM4CTC

The breakdown of hexagonal symmetry of the pyrimidine ring is obvious from the shortening of C₁₄-N₁₈ (~0.104 Å) and C₁₆-N₂₀ (~0.090 Å) due to the substitution of oxo group to the ring. There is an elongation of C₂₂-Cl₂₅ bond length (~0.065Å), C₂₆-O₂₈ bond length (~0.146Å) and C₂₄-O₂₇ bond length (~0.012Å) due to the substitution of chloro methyl group and carboxylate group to the pyrimidine ring.

The asymmetry of the pyrimidine ring is also evident from the negative deviation of C₁₂-C₁₃-C₁₆ (118.58°) and positive deviation of N₁₈-C₁₄-O₁₉ (125.32°) from the normal value of 120°. The carbon atoms usually take two types of hybridization SP² and SP³ when they are in rings, with bond angle 120° and 109°, respectively. In this molecule, for many of the bond angles around carbon show the values in the range 118° to 121° both in phenyl and pyrimidine rings which shows the deviation from the SP³ hybridization at these atoms. At H₂₃-C₂₂-H₂₄, H₂₃-C₂₂-Cl₂₅ and H₂₄-C₂₂-Cl₂₅ the bond angles are 109.93°, 105.55°, 106.98°, respectively, this shows the deviation from the SP² hybridization. It also indicates that the SP³ takes place when there is an H atom on one side of the carbon atom. All these deviation from the ideal angles 120° and 109° indicate that the regular hexagonal structure is distorted due to the substitution groups and presence of N atoms in the pyrimidine group.

NLO Property

Organic and semi-organic NLO materials have been subjected to the intense of research, due to their possible application in a wide range of technologies, such as optical communication, optical computing and data storage, [Geskin *et al.*, 2003, Nakano *et al.*, 2002 and Sajjan *et al.*, 2006]. The first order hyperpolarizability is a third rank tensor that can be described by a 3x3x3 matrix. The 27 components of the 3D matrix can be reduced to 10 components due to Kleinman symmetry [Kleinman, 1962] The total static dipole moment (μ), the mean polarizability (α_0) and the mean first order hyperpolarizability (β_0), using the x, y, z components are defined as

$$\mu = (\mu_x^2 + \mu_y^2 + \mu_z^2)^{1/2} \quad (1)$$

$$\alpha_0 = \frac{\alpha_{xx} + \alpha_{yy} + \alpha_{zz}}{3} \quad (2)$$

$$\alpha_0 = \frac{\alpha_{xx} + \alpha_{yy} + \alpha_{zz}}{3} \quad (3)$$

The NLO properties of ECM4CTC have been calculated using B3LYP/6-311++G(d,p) method. The dipole moment (μ) and first order hyperpolarizability (β_0) values are calculated at 1.79560 Debye and 6.60035 x 10⁻³⁰ esu, respectively. The first order hyperpolarizability (β_0) of the title compound is eighteen times greater than that of standard urea (μ = 1.3732 Debye, β_0 = 0.3728 x 10⁻³⁰ esu), hence the molecule has good NLO activity. The dipole moment and first order hyperpolarizability of ECM4CTC are given in Table. 2. From the table, it is found that both the dipole moment and first order hyperpolarizability of the molecule are greater in x and y direction than in z direction.

NBO Analysis

The bonding and anti-bonding interactions can be quantitatively described in terms of the NBO analysis, which is expressed by means of the second-order perturbation interaction energy ($E^{(2)}$) [Reed, 1985, Foster, 1980,

Chocholousova 2004 and Fleming 1976]. This energy represents the estimate of the off-diagonal Fock matrix elements. It can be deduced from the second-order perturbation approach [Foster *et al.*, 1980] as

$$E^{(2)} = \Delta E_{ij} = q_i \frac{F(i, j)^2}{\epsilon_j - \epsilon_i} \quad (4)$$

where q_i is the donor orbital occupancy, Σ_i and Σ_j are diagonal elements (orbital energies) and F(i,j) is the off diagonal NBO Fock matrix elements.

Table 2 The molecular electric dipole moments (μ), polarizability (α_0) and hyperpolarizability (β_0) values of ECM4CTC

Parameters	B3LYP/6-311++G(d,p)
Dipole moment (μ)	
μ_x	1.3746753
μ_y	1.1394275
μ_z	-0.1901876
μ	1.79560Debye
Hyperpolarizability (β_0)	
β_{xxx}	486.2019507
β_{xyx}	-189.5549425
β_{xyy}	168.2445594
β_{yyy}	528.8730644
β_{xxx}	-87.0757176
β_{xyz}	-64.7310125
β_{yyz}	6.4590761
β_{xzz}	49.3528490
β_{yzz}	-65.0252389
β_{zzz}	-33.8954170
β_0	6.60035x10 ⁻³⁰ esu

Standard value for urea (μ =1.3732 Debye, β_0 =0.3728x10⁻³⁰esu): esu-electrostatic unit.

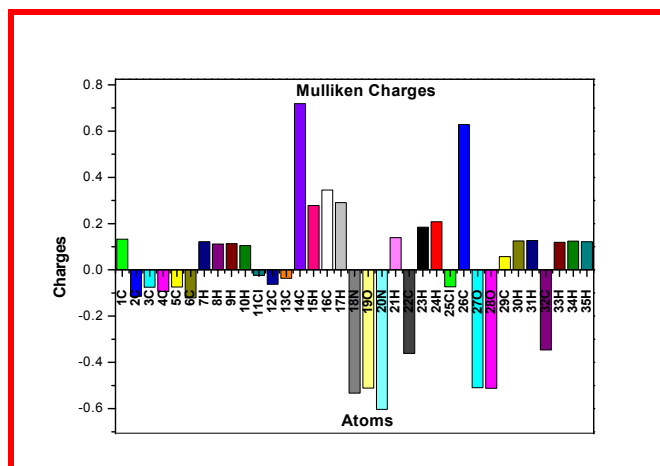


Fig 6 Mulliken atomic charges plot of ECM4CTC

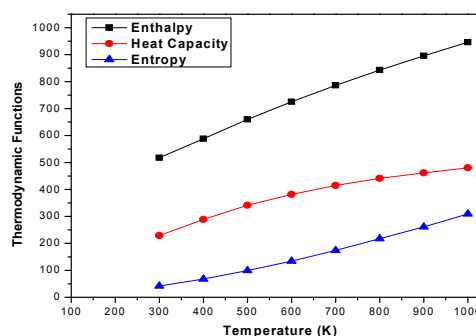


Fig. 7. The Thermodynamic properties at different temperatures of ECM4CTC

Table 3 The Second order perturbation theory analysis of Fock Matrix in NBO basis for ECM4CTC

Type	Donor NBO (i)	ED/e	Acceptor NBO (j)	ED/e	^a E ⁽²⁾ KJ/mol	^b E(j)-E(i) a.u.	^c F(i,j) a.u.
$\pi-\pi^*$	BD (2) C1-C2	1.64622	BD*(2) C3 - C4	0.38909	91.46	0.27	0.069
			BD*(2) C5 - C6	0.32295	87.53	0.28	0.069
$\pi-\pi^*$	BD (2) C3-C4	1.67636	BD*(2) C1 - C2	0.34713	78.58	0.3	0.067
			BD*(2) C5 - C6	0.32295	81.84	0.3	0.068
$\pi-\pi^*$	BD (2) C5-C6	1.67007	BD*(2) C1 - C2	0.34713	81.96	0.29	0.067
			BD*(2) C3 - C4	0.38909	86.02	0.27	0.068
$\pi-\pi^*$	BD (2) C26-O27	1.97902	BD*(2) C13 - C16	0.23132	20.84	0.4	0.042
$n-\sigma^*$	LP (2) Cl11	1.97342	BD*(1) C3 - C4	0.02671	15.98	0.88	0.052
			BD*(1) C4 - C5	0.02668	16.07	0.88	0.052
$n-\pi^*$	LP (3) Cl11	1.93185	BD*(2) C3 - C4	0.38909	50.04	0.33	0.061
$n-\sigma^*$	LP (1) N18	1.74362	BD*(1) C1 - C12	0.04556	32.97	0.66	0.068
			BD*(1) C14 - O19	0.0392	11.63	0.83	0.045
			BD*(2) C14 - O19	0.33641	190.08	0.32	0.11
$n-\sigma^*$	LP (2) O19	1.84384	BD*(1) C14 - N18	0.07443	103.6	0.7	0.12
			BD*(1) C14 - N20	0.08937	117.61	0.65	0.123
$n-\pi^*$	LP (1) N20	1.67259	BD*(2) C13 - C16	0.23132	173.72	0.3	0.102
			BD*(2) C14 - O19	0.33641	182.84	0.33	0.107
$n-\sigma^*$	LP (2) Cl25	1.98337	BD*(1) C22 - H23	0.01743	11.63	0.76	0.041
$n-\sigma^*$	LP (1) O27	1.97517	BD*(1) C13 - C26	0.0584	11.76	1.13	0.051
$n-\sigma^*$	LP (2) O27	1.85039	BD*(1) C13 - C26	0.0584	72.51	0.7	0.101
			BD*(1) C26 - O28	0.09842	136.31	0.63	0.129
$n-\sigma^*$	LP (1) O28	1.95658	BD*(1) C22 - H24	0.01939	13.64	1.05	0.053
			BD*(1) C26 - O27	0.01749	30.5	1.16	0.082
$n-\pi^*$	LP (2) O28	1.80738	BD*(2) C26 - O27	0.29837	193.01	0.33	0.113
$\pi^*-\pi^*$	BD*(2) C3-C 4	0.38909	BD*(2) C1 - C2	0.34713	754.92	0.02	0.084
			BD*(2) C5 - C6	0.32295	921.07	0.01	0.08
$\pi^*-\pi^*$	BD*(2) C26-O27	0.29837	BD*(2) C13-C16	0.23132	334.97	0.02	0.076

^a E⁽²⁾ means energy of hyper conjugative interaction (stabilization energy).

^b Energy difference between donor (i) and acceptor (j) nbo orbitals.

^c F(i,j) is the Fock matrix element between i and j nbo orbitals.

In this study, the charges transferring from bonding to anti-bonding level has been analyzed. The intra-molecular hyper conjugative interactions are caused by the orbital overlapping between $\pi-\pi^*$ bonds in the chloro phenyl ring $\pi(C_1-C_2)/1.64622$ ED/e to $\pi^*(C_3-C_4)$, (C_5-C_6) which leads to give a Stabilization energy of 91.46 and 87.53 KJ/mol, respectively. Similarly, $\pi(C_5-C_6)/1.67007$ ED/e interacts with $\pi^*(C_1-C_2)$, (C_3-C_4) to give a Stabilization energy of 81.96 and 86.02 KJ/mol.

The electron density and delocalization energies of ECM4CTC are given in Table 3. The maximum charge delocalization occurs from the lone pairs of electrons. The molecule ECM4CTC contains lone pairs of electrons on oxygen and nitrogen atoms which results in intra-molecular charge transfer (ICT) causing stabilization of the molecular system. These lone pairs on N₁₈ (1.74362 ED/e) and O₂₈ (1.80738 ED/e) atoms gave a maximum energy transfer to $\pi^*(C_{14}-O_{19})/190.08$ and $\pi^*(C_{26}-O_{27})/193.01$ KJ/mol, respectively.

In hetero cyclic atoms, the maximum hyper conjugative E⁽²⁾ energy exhibited during the inter-molecular interaction, which leads the molecule towards medicinal and biological application. According to the stabilization energy values, the first five most probable electronic transitions in this molecule in the descending order are: 1. C₃ - C₄ to C₅ - C₆ ($\pi^*-\pi^*$ and E² = 921.07), 2. C₃ - C₄ to C₅ - C₆ ($\pi^*-\pi^*$ and E² = 754.92), 3. LP (1) O₂₈ to C₂₆ - O₂₇ ($n-\pi^*$, E² = 193.01), 4. LP (1) N₁₈ to C₁₄ - O₁₉ ($n-\pi^*$, E² = 190.08), and 5. LP (1) N₂₀ to C₁₄ - O₁₉ ($n-\pi^*$, E² = 182.84). But among the five most probable transitions, only one or two will take place with high intensity which can be observed in the experimental UV-Visible spectrum also, whose values are determined by the high oscillator strength which can be calculated from HOMO- LUMO analysis.

HOMO-LUMO Analysis

The highest occupied molecular orbital (HOMO) and the lowest unoccupied molecular orbital (LUMO) are named as frontier molecular orbitals (FMOs). The FMOs play an important role in the optical and electronic properties [Fleming, 1976]. The frontier molecular orbital compositions of ECM4CTC are shown in Fig. 2. In this study, the HOMO is located over the tetrahydropyrimidine ring. But, Lumo is occupied at whole molecule except ethyl group.

Gauss-Sum 2.2 Program [O'Boyle *et al.*, 2008] was used to calculate group contributions to the molecular orbitals (HOMO and LUMO) and the density of the state (DOS) as shown in Fig. 3. The spectrum is used to explain the contribution of electrons to the conduction and valence band. The spectrum gives idea about how many states are available at certain energy states. The lines at the starting end of the energy axis of the plot that is from -20 Ev to -5 Ev, are called filled orbital and from -5 Ev to 0 Ev, are called virtual orbital. The virtual orbital are not occupied and are also called acceptor orbital, whereas the filled orbital are called donor orbital. A high intensity DOS at a specific energy levels means that there are many states available for occupation. A DOS of zero intensity means that no states can be occupied by the system. The variation in the peak height is due to the movement of electrons between the C=C and C-C in the ring of the molecule.

HOMO and LUMO energies are predicted as -6.504 eV and -1.771 eV, respectively. The HOMO and LUMO energy gap is 4.733 eV, which explains the eventual charge transfer interactions taking place within the molecule. The global chemical reactivity descriptors such as hardness (η), softness (S), chemical potential (μ), electrophilicity index (ω) and electronegativity (χ) are calculated using HOMO and LUMO

energy values and are listed in Table 4. In addition the kinetic energies of the ECM4CTC molecule are listed in Table 5. The energy values of HOMO (π -donor) and LUMO (π -acceptor) and their energy gap reflects the chemical activity of the molecule. The energy gap between HOMO and LUMO has been used to prove the Bio-activity from intra molecular charge transfer (ICT) [Sagdinc *et al.*, 2009].

Table 4 The Physico-chemical properties of ECM4CTC

Parameters	Values
HOMO	-6.504eV
LUMO	-1.771 eV
Energy gap	4.733 eV
Ionization potential (IP)	6.504 eV
Electron affinity (EA)	1.771eV
Electrophilicity Index (ω)	3.617
Chemical Potential (μ)	-4.138
Electronegativity (χ)	4.138
Hardness (η)	2.367
Softness (S)	0.211

Table 5 The frontier molecular orbitals energies of ECM4CTC

Orbitals	Energies (a.u)	Energies (eV)	Kinetic Energies (a.u)
Homo-4	-0.280	-7.622	2.282
Homo-3	-0.269	-7.306	2.035
Homo-2	-0.263	-7.152	1.214
Homo-1	-0.246	-6.687	1.633
Homo	-0.239	-6.503	1.645
Energy gap	0.174	4.733	
Lumo	-0.065	-1.770	1.885
Lumo+1	-0.016	-0.426	1.443
Lumo+2	-0.014	-0.382	1.487
Lumo+3	0.006	0.150	2.216
Lumo+4	0.030	0.818	2.105

UV-Vis Analysis

To obtain the nature of the transitions, electronic excitation energies and oscillatory strength the UV-Visible spectrum of ECM4CTC in gas phase has been studied by the time-dependent functional theory (TD-SCF). The observed and calculated electronic transitions of highest oscillator strength are given in Table 6.

Table 6 The electronic transition of ECM4CTC using B3LYP/6-311++G(d,p) basis set

Calculated at B3LYP/6-311++G(d,p)	Oscillator strength	Calculated Band gap (eV/nm)	Experimental Band gap (eV/nm)	Type
Excited State-1	Singlet- $\Lambda(f=0.0626)$	3.8193eV/324.63nm	340	$n-\pi^*$
84 \rightarrow 86	-0.1264			
85 \rightarrow 86	0.6348			
85 \rightarrow 89	-0.1056			
Excited State-2	Singlet- $\Lambda(f=0.0085)$	3.9809eV/311.45nm	290	$n-\pi^*$
80 \rightarrow 86	0.2231			
83 \rightarrow 86	0.1106			
84 \rightarrow 86	0.6311			
85 \rightarrow 86	0.1015			
Excited State-3	Singlet- $\Lambda(f=0.0056)$	4.6550eV/266.34nm	220	$\pi-\pi^*$
80 \rightarrow 86	0.2085			
83 \rightarrow 86	0.6209			
84 \rightarrow 86	-0.1881			

The UV-Vis absorption spectrum of ECM4CTC is recorded in the range 200-800 nm. The experimental and theoretical UV-Vis spectrum is shown in Fig. 4. The three intense calculated electronic transitions at $\lambda_{max} = 324.63$ nm, $f = 0.0626$; $\lambda_{max} =$

311.45 nm, $f = 0.0085$ and $\lambda_{max} = 266.34$ nm, $f = 0.0056$ have been obtained which corresponds values at 340, 290 and 220 nm, respectively. Of these three electronic transitions, only the first transition has relatively high intensity as the oscillator strength gives the measure of intensity. The other two have lower intensity with respect to the first one. As the first two wave numbers for these transitions lie in the $n-\pi^*$ transitions; they can be LP(1)O28 to C26 - O27 ($n-\pi^*$, $E2 = 193.01$), LP(1)N18 to C14 - O19 ($n-\pi^*$, $E2 = 190.08$), and the third one is C1 - C2 to C3 - C4 ($\pi-\pi^*$ and $E2 = 91.46$), which belong to $\pi-\pi^*$ transition.

MEP Surfaces

The molecular electrostatic potential (MEP) is related to the electron density and is a very useful descriptor in understanding sites for electrophilic and nucleophilic reactions as well as hydrogen bonding interactions [Scrocco *et al.*, 1979 and Luque *et al.*, 2000]. The MEP plot for the ECM4CTC molecule calculated by DFT/B3LYP/6-311++G(d,p) method. The different values of MEP surface are represented by different colors: red, blue and green represent the regions of most negative, most positive and zero electrostatic potential, respectively. The red colour represents negative electrostatic potential corresponds to an attraction of the proton by the aggregate electron density in the molecule, while the positive electrostatic potential corresponds to a repulsion of the proton by the atomic nuclei (blue). From the MEP surface is evident that the negative charge covers the C=O group and the positive region is over the hydrogen atoms in ECM4CTC molecule. The total density, alpha density, ESP and MEP surface of the title molecule is shown in Fig. 5.

Mulliken Charges

The prediction of atomic charges is important as they determine the dipole moment, polarizability, bond strength, vibrational frequencies, and electronic transitional energy levels and so on in any molecular system. The atomic charges of ECM4CTC are calculated by Mulliken population analysis method with B3LYP functional and 6-311++G(d,p) basis set and the values are listed in Table 7.

Table 7 The Mulliken atomic charges of ECM4CTC

Atoms	Charges(a.u)	Atoms	Charges(a.u)
1C	0.1328	19O	-0.5114
2C	-0.1144	20N	-0.603
3C	-0.0748	21H	0.1398
4C	-0.0934	22C	-0.3615
5C	-0.0742	23H	0.1842
6C	-0.1209	24H	0.2077
7H	0.1221	25Cl	-0.0737
8H	0.1113	26C	0.6280
9H	0.1130	27O	-0.5092
10H	0.1052	28O	-0.5123
11Cl	-0.0240	29C	0.0574
12C	-0.0628	30H	0.1251
13C	-0.0361	31H	0.1266
14C	0.7184	32C	-0.3461
15H	0.2786	33H	0.1195
16C	0.3450	34H	0.1244
17H	0.2906	35H	0.1217
18N	-0.5332		

The graphical representation of the same is shown in Fig. 6. From the results, N₁₈ atom shows the higher negative charge. The C₁₄ atom has high positive charge due to the attachment of carbonyl group (C₁₄=O₁₇). In the phenyl ring, all the carbon

atoms are expected to be equally negative around -0.1 a.u, this is almost observed for all carbon atoms in the benzene ring except for C₁, where the pyrimidine ring is attached. That shows pyrimidine ring is more electronegative when comparing to benzene, which is naturally due to the presence of N atoms in the ring.

In the case of Pyrimidine ring, the carbon atoms C₁₂ and C₁₃ are negative while C₁₄ and C₁₆ are positive; this shows the large asymmetrical charge distribution in the ring, due to the presence of two N atoms inside the ring, which is also the reason for different type of conjugation in this ring. The C₄ and C₂₂ atoms are attached with chlorine atom Cl₁₁ and Cl₂₅ in adjacent positions. Due to the presence of lone pair of electrons on chlorine atoms, the C₄ and C₂₂ atoms have more negative charge among the other carbon atoms. All the hydrogen atoms have equal positive charge around 0.1a.u, which shows that their electrons are partially shifted towards the carbon atoms with which they get attached and they are not disturbed by the various substitutional groups.

Thermodynamic Properties

On the basis of vibrational analysis at B3LYP/6-311++G(d,p) level of calculation, the standard thermodynamic functions: heat capacity (C_{p,m}⁰), entropy (S_m⁰) and enthalpy changes (H_m⁰) for the ECM4CTC were obtained from the theoretical harmonic frequencies and are listed in Table 8.

Table 8 The Thermodynamic properties at different temperatures of ECM4CTC

T (K)	S _m ⁰ (J/mol.K)	C _{p,m} ⁰ (J/mol.K)	H _m ⁰ (KJ/mol)
100	341.08	104.22	8.76
200	427.16	157.75	21.97
298.15	515.87	216.56	40.74
300	517.37	228.75	42.13
400	587.94	288.39	67.88
500	659.78	341.57	99.27
600	725.28	381.39	134.26
700	786.23	414.84	173.89
800	843.07	441.08	217.35
900	895.86	461.55	261.29
1000	946.26	480.47	309.16

It can be observed that these thermodynamic functions are increasing with temperature ranging from 100 to 1000 K due to the increase in vibrational intensities with temperature and also due to increase in equipartition energy with increase in temperature [Sajan *et al.* 2011]. The correlation graphs of thermodynamic properties and its functions (heat capacity, entropy and enthalpy changes) are shown in Fig. 7.

All the thermodynamic data are supportive information for further study on the molecule. They can be used to compute other thermodynamic functions using the standard thermodynamical relationship, which may be used to find out the other physical and chemical properties [Zhang *et al.*, 2011].

Vibrational Assignments

The title molecule possesses C₁ point group symmetry and 99 normal modes of vibrations are distributed into two types, such as A' (in-plane bending vibrations) and A'' (out-of-plane bending vibrations). The irreducible representation for the C₁ symmetry is given by $\Gamma_{\text{vib}} = 67 A' + 32 A''$. All the vibrations are found active collectively in both IR and Raman spectra, which are shown in Fig. 8 and Fig. 9, respectively. The theoretically predicted wavenumbers, experimental wave numbers and assignments along with their TED values are

presented in Table 9. Scaling strategies were used to bring computed wave numbers closer to the observed values. In this study, the scaling factor used is 0.9608 as advised by the earlier work [Rauhut *et al.*, 1995]. Hence, the calculated wave numbers, which are scaled by suitable factor, are found in good agreement with experimental wavenumbers.

C-H Vibrations

In General, the aromatic C-H stretching vibrations occur in the region of 3100-3000 cm⁻¹ [Sharma, 1994]. In this study, there are four C-H stretching vibrations of chloro phenyl group which are assigned at 3151, 3116, 3115, 3103 cm⁻¹ respectively. The band observed at 3123 cm⁻¹ in FT-IR, 3125 cm⁻¹ in FT-Raman spectrum is assigned to ν C-H vibration of chloro phenyl group. The scaled harmonic frequencies in the range 3010-2954 cm⁻¹ (mode nos: 10 to 14) are attributed to C-H stretching vibrations of carboxylate group attached to the pyrimidine ring in ECM4CTC. In addition, the ν C-H vibration of carboxylate group is observed at 2975 cm⁻¹/FT-IR and 2978 cm⁻¹/ FT-Raman and the harmonic wave number lies at 2971 cm⁻¹. These results are considerable as pure mode of vibrations with TED 99%. But only one mode is observed in both FT-IR and FT-Raman spectrum (mode 13). Also three of these vibrations are in the lower range due to the impact of O atom in the carboxylate group. The pure mode of scaled wavenumber 3035 cm⁻¹ (mode 8) with TED 99% contribution is due to the C-H stretching vibration of the pyrimidine ring. All the C-H stretching vibrations of the pyrimidine ring are missing in both the spectrum, due to the substitution of chloro phenyl group in the adjacent position.

The theoretically calculated unscaled values of C-H in-plane bending vibrations of phenyl ring vibrations fall in the region 1214-1184 cm⁻¹ (mode nos: 39 to 42). Of which, two are observed in FT-IR spectra with wave numbers 1171 and 1137 cm⁻¹ (mode no. 39 & 42). Similarly the harmonic bands due to C-H out-of-plane bending vibration fall in the region 593-513 cm⁻¹ (mode nos: 70 to 73). In this study, some of the experimental bands are missing for β_{CH} and τ_{CH} modes, which may be due to the steric factor of bulky group (pyrimidine ring). The β_{CH} and τ_{CH} modes are within the expected region with few exceptions and also having considerable TED values: >60 and mode no: 70 and 71 are a pure torsion mode with TED 65% and 73%, respectively.

C-Cl Vibrations

Generally, the C-Cl stretching vibrations are strong bands at the region of 760- 505 cm⁻¹. This vibration due to a chlorine atom is worth to discuss, as there is mixing of the vibrations possible due to lowering of the molecular symmetry and the presence of heavy atom [Chithambarathanu *et al.*, 2002 and Dhandapani *et al.*] reported the ν C-Cl stretching vibration at 725 cm⁻¹ FT-Raman spectrum. In our case, the ν C-Cl band of chloro phenyl ring is observed at 770 cm⁻¹ in FT-IR with 56% TED/Mode No. 61 and 750 cm⁻¹ in FT-Raman with 60% TED/Mode No. 62. The corresponding theoretical wave number lies at 776 and 744 cm⁻¹ respectively. These values are good agreement with literature. Sundaraganesan *et al.* reported the C-Cl in-plane and out-of-plane bending deformation bands at 250 and 160 cm⁻¹, respectively [Sharma, 1994]. In this study, the C-Cl in-plane bending vibrations of chloro phenyl ring were calculated at 860 and 698 cm⁻¹ and that of chloro methyl group at 1151,656 cm⁻¹. Similarly, the C-Cl out-plane bending vibrations of chloro methyl ring and that of chloro

phenyl group were calculated at 444 and 55 cm^{-1} respectively. The C-Cl in-plane and out-plane bending vibrations of chloro methyl ring occur in the higher wave number, because of presence of pyrimidine ring in adjacent position.

C-N Vibrations

Generally, the C=N/C-N stretching vibrations were observed in the regions of 1600-1670 cm^{-1} /1266-1382 cm^{-1} respectively. Khalaji *et al.* reported that the C=N (aromatic) stretching mode in the region 1490-1570 cm^{-1} . Since mixing of bands is possible in the region 1400-1200 cm^{-1} , the stretching of C-N group identification is a difficult task. For the title molecules, the four CN stretching vibrations are identified with the help of TED, they are assigned at harmonic wavenumbers 1502, 1487, 1450, 1407 cm^{-1} (mode nos: 23, 24, 27, 30). The observed bands occurred in FTIR spectra at 1457, in FT-Raman at 1365 cm^{-1} respectively. The assigned CN stretching modes indicate that all of them are C-N modes rather than C=N modes, which shows there is no double bonded CN within the pyrimidine ring. The in-plane bending vibrations: $\beta\text{C}_{14}\text{C}_{16}\text{N}_{20}$; $\beta\text{C}_{14}\text{C}_{16}\text{N}_{20}$; $\beta\text{C}_{14}\text{C}_{16}\text{N}_{20}$; $\beta\text{C}_{12}\text{C}_{13}\text{N}_{18}$; $\beta\text{N}_{16}\text{C}_{14}\text{N}_{18}$ are attributed to mode nos: 30, 58, 64 and 57 respectively. The respective experimental $\beta\text{C}_{14}\text{C}_{16}\text{N}_{20}$ value is 1365 cm^{-1} . The out-of-plane bending mode of $\Gamma_{\text{C-N}}$ contributes as mixed vibrations of $\Gamma\text{N}_{18}\text{C}_{12}\text{C}_{14}\text{H}_{15}$ (mode no 68) and pure vibration of $\Gamma\text{C}_{12}\text{C}_{13}\text{H}_{21}$ (mode no 75). The corresponding observed wave numbers in FT-Raman were 625, 452 cm^{-1} .

N-H Vibrations

The N-H stretching vibrations are expected to appear in the region of 3500-3300 cm^{-1} for heterocyclic molecules [Barthes *et al.*, 1996]. In this study, the wave numbers 3512, 3509 cm^{-1} are assigned to this modes, the peak observed at 3505 cm^{-1} in FT-IR represent the N-H stretching mode with 93% TED. This observed wave number is negatively 125 cm^{-1} deviated from harmonic frequencies, which is due to the presence of moderate anharmonicity in this vibration. In addition, the in-plane bending vibrations observed at 1250 cm^{-1} in FT-Raman spectrum with $\beta\text{H}_{15}\text{N}_{18}\text{C}_{14}(63)+\beta\text{H}_{15}\text{N}_{18}\text{C}_{12}(23)$ mixed vibrations at Mode no. 37 and its corresponding harmonic value at 1252 cm^{-1} . The N-H out-plane and torsional mode $\tau\text{H}_{15}\text{N}_{18}\text{C}_{14}\text{N}_{20}(62)+\Gamma\text{N}_{18}\text{C}_{12}\text{C}_{14}\text{H}_{15}(27)$ is assigned at 625 in FT-Raman and for the same mode the corresponding harmonic values are 643 cm^{-1} (mode nos: 68). Similarly the $\tau\text{H}_{17}\text{N}_{20}\text{C}_{16}\text{C}_{22}(76)+\Gamma\text{N}_{20}\text{C}_{14}\text{C}_{16}\text{H}_{17}(16)$ mode is calculated at 636 cm^{-1} (mode nos: 69).

C=O and C-O Vibrations

Generally, the C=O stretching vibrations are expected in the region of 1715-1600 cm^{-1} , it is moderately intense in IR and Raman spectra [Roeges, 1994]. In this case, the $\text{O}_{27}\text{C}_{26}$ stretching band shows strong peak at 1694 cm^{-1} in FT-IR and 1695 cm^{-1} in FT-Raman, and its equivalent wave number computed is 1697 cm^{-1} with 86% TED at Mode no. 16. The oxo group C=O stretching vibration was computed at 1832 cm^{-1} (mode no. 15) and it is shifted to higher wave number, due to the presence of chlorine in chloro methyl group. The C-O stretching vibrations usually occur in the region 1260-1000 cm^{-1} [Varsanyi, 1969]. The C-O band observed at 1090 cm^{-1} (FT-IR) is assigned to $\nu\text{O}_{28}\text{-C}_{29}$ (54%). The ester group C-O stretching vibration was computed at 1076 cm^{-1} (mode no. 46).

Ring Vibrations

The ring vibration includes C=C and C-C vibrations. The C=C stretching vibrations are expected in the region 1625-1430 cm^{-1} [Mohan, 2001]. In the phenyl ring, the six carbon atoms undergo coupled vibrations called skeletal vibration or ring

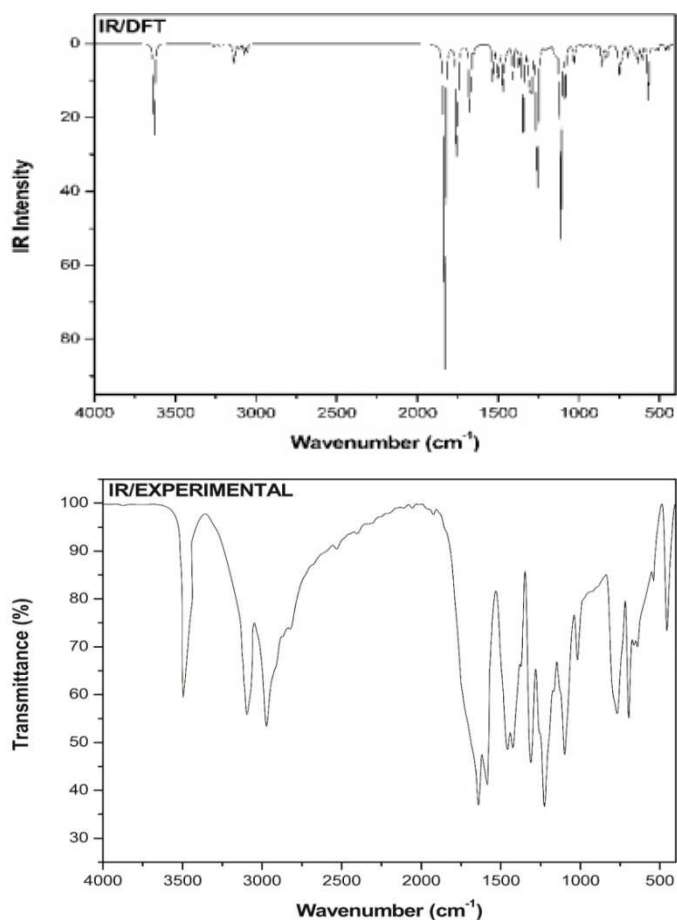


Fig 8. Theoretical and Experimental FT-IR Spectra of ECM4CTC

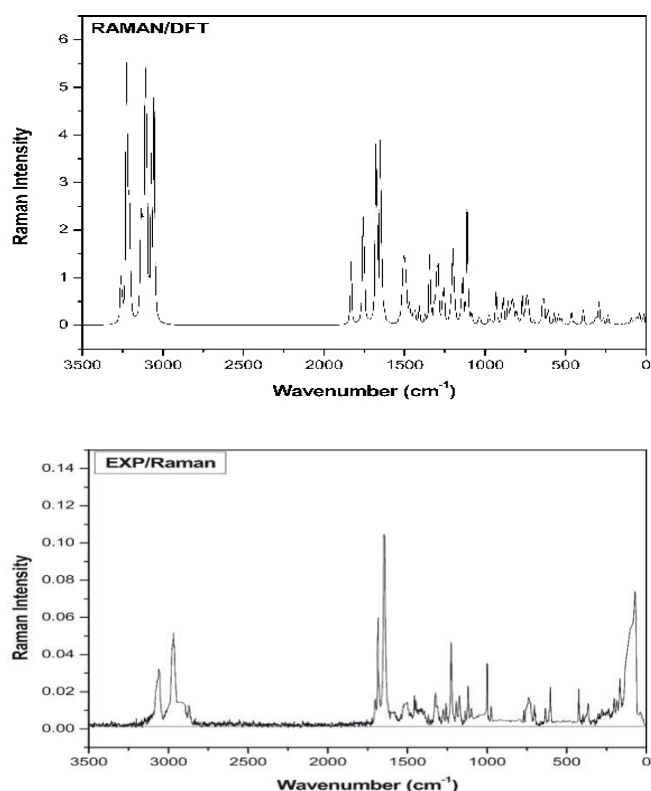


Fig 9 The Theoretical and Experimental FT-Raman Spectra of ECM4CTC

vibration. In our case, the bands observed at 1489 cm^{-1} in FT-IR and 1575, 1490 cm^{-1} in FT-Raman spectrum are assigned to C=C stretching vibrations, the modes were calculated at 1627, 1482 cm^{-1} (Mode No. 19,20/ TED: 39, 63%) respectively. This result is in good agreement with literature.

The theoretically calculated $\nu_{\text{C-C}}$ modes: 1675, 1439, 1411, 1344 & 1334 cm^{-1} (mode nos: 17, 28, 29, 32, 33) of the pyrimidine ring have been obtained to be consistent with the recorded spectral values: 1630, 1305 cm^{-1} (FTIR bands) and 1625 cm^{-1} (FT-Raman). The theoretically computed β_{CCC} wave numbers of phenyl ring by DFT method are at 960, 931, 889, 860 cm^{-1} (modes : 53 to 56) respectively [Roeges, 1994]. The corresponding experimental spectra are absent, due to the presence of chlorine on the phenyl ring. The modes: 82 to 85 respectively were recognized as torsional deformation τ_{CCC} modes. The harmonic wave numbers of β_{CCC} , Γ_{CCC} and τ_{CCC} modes of pyrimidine ring were computed at 803, 752 and 464, 268 cm^{-1} , respectively. The respective experimental wave numbers β_{CCC} and Γ_{CCC} were occurred at 770 (FT-IR), 452 (FT-Raman) cm^{-1} . These harmonic wave numbers are shifted to the lower range due to the presence of chloro phenyl, carboxylate group and chloro methyl group to the tetra hydro perimidine ring. According to TED results the β_{CCC} and Γ_{CCC} vibrations are mixed with β_{CCH} , β_{CCN} and Γ_{CCH} modes of the neighbouring group.

Methyl group vibrations

The compound ECM4CTC contains one CH_2Cl group attached to pyrimidine ring. In CH_2Cl , the C-H stretching occurs at lesser frequencies than those of aromatic C-H stretching (3100-3000 cm^{-1}). The region around 2980 cm^{-1} is assigned to asymmetric C-H stretching mode of CH_2Cl group [Clouthup *et al.*, 1990, Kleinman, 1990, Smith *et al.*, 1999 and Socrates, 1990] and the region around 2870 cm^{-1} is allotted to symmetric C-H stretching mode. In asymmetric stretching of CH_3 mode, the two C-H bonds of the methyl group are expanding while the third one is contracting. In symmetric stretching of CH_3 mode, all the three C-H bonds expand and contract in-phase. The asymmetric stretching for the CH_3 has higher magnitude than the symmetric stretching [Sudha *et al.*, 2011, Varsanyi, 1969 and Socrates, 1980]. In ECM4CTC, the $\text{C}_{22}\text{-H}_{24}$ and $\text{C}_{22}\text{-H}_{23}$ of symmetric and asymmetric stretching vibrations of methyl group did not occur in both FT-IR and FT-Raman region. The expected theoretically values obtained by B3LYP/6-311++G(d,p) method at 3205, 3132 cm^{-1} (mode nos: 7, 9). The substitution of chlorine atom to methyl group has affected the C-H vibration to higher value. The $\beta_{\text{H}_{23}\text{C}_{22}\text{H}_{24}}$ was calculated at 1151 cm^{-1} with TED 64% and $\beta_{\text{H}_{23}\text{C}_{22}\text{C}_{16}}$ at 1137 cm^{-1} with TED 57%.

CONCLUSION

The optimized structural parameter such as bond length, bond angle and dihedral angles are also calculated using DFT/B3LYP/6-311++G(d,p) method and also compared with reported XRD values. The conjugative system posses more Non-linear optical behavior, it also provides the evident from first order hyperpolarizabilities. NBO analysis reflects the charge transfer occur within the molecule. The Lewis and non-Lewis structure of ECM4CTC shows that the contribution of ED of individual atoms, which leads the molecular vibration with respect to hybridization of chemical bonds. HOMO and LUMO orbitals have been visualized. The lowering of HOMO

and LUMO energy gap supports the bioactivity property of the molecule. The MEP map shows the negative potential sites are on oxygen and nitrogen atoms as well as the positive potential sites are around the hydrogen atoms. Mulliken charges analyzed positive and negative charges atoms (C_{14} and N_{20}) are presented in tetrahydropyrimidine ring. The thermodynamic properties at different temperatures of ECM4CTC molecule have been calculated and analyzed. Finally, the complete vibrational assignments of ECM4CTC analyzed with the help of TED contribution. The electronic features, such as absorption wavelength (λ), excitation energies (E), oscillator strengths (f) have been investigated by experimental and theoretical methods. We hope the results of this study will help researchers to design new drugs and materials. This can also assist experimental chemist to find entirely new chemical objects.

References

- Barthes, M., DeNunzio, Gand Ribet, G., *Synth. Met.*, 76 (1996) 337-340.
- Bharanidharan, S., Saleem, H., Gunasekaran, B., Syed Ali Padusha, M., Suresh, M. Crystal structure of ethyl 6-(chloromethyl)-4-(4-chlorophenyl)-2-oxo-1,2,3,4-tetrahydropyrimidine-5-carboxylate, *Acta Cryst.* 2014, E70, o1185-o1186.
- Beena, K.P., Akelesh, T. *Int. Res. J. Pharm.* 2012, 3, 303-304.
- Bist, H.D., Brand, J.C.D., Williams, D.R. *J. Mol. Spectrosc.* 1967, 24, 402-412.
- Chithambarathanu, T., Umayorubagan, V and Krishnakumar, V., *Indian J. Pure Appl. Phys.*, 40 (2002) 72-74.
- Chocholoušová, J., Špirko, V., & Hobza, P. First local minimum of the formic acid dimer exhibits simultaneously red-shifted O-H...O and improper blue-shifted C-H...O hydrogen, *Physical Chemistry Chemical Physics*, 2004, 6(1), 37-41
- Coluthup, N.B., Paly, L.H., Wiberley, S.E. Introduction to Infrared and Raman Spectroscopy, third ed., Academic press, Boston, MA, 1990.
- Dhandapani, A., Manivarman, S., Subashchandrabose, S., *Chem. Phys. Lett.* (2016), [http:// dx.doi.org/10.1016/j.cplett.2016.04.009](http://dx.doi.org/10.1016/j.cplett.2016.04.009).
- Evans, J.C. *Spectrochim. Acta.* 1960, 16, 1382-1392.
- Fedorova, O.V., Zhidovinova, M.S., Rusinov, G.L., Ovchinnikova, I.G. *Russ. Chem. Bull. Int. Ed.* 2003, 52, 1768-1769.
- Fleming, I., *Frontier Orbitals and Organic Chemical Reactions*, Wiley, London, 1976.
- Frisch, M.J., Pople, J.A. *Gaussian 03, Revision C.02*, Gaussian Inc., Wallingford, CT, 2004.
- Foster, J.P., Wienhold, F. *J. Am. Chem. Soc.* 1980, 102, 7211-7218.
- Geskin, V.M., Lambert, C.J., Bredas, L. Origin of high second and third-order nonlinear optical response in ammonio/borato diphenylpolyene zwitterions: the remarkable role of polarized aromatic groups, *J. Am. Chem. Soc.* 125 (2003) 15651-15658.
- Jamroz, M.H. *Vibrational Energy Distribution Analysis: VEDA4 program*, Warsaw, Poland, 2004.
- Kleinman, D.A., (1962). *Nonlinear Dielectric Polarization in Optical Media*, Physics Reviews, 126, 1977-1979.

- Kleiman, D.A. *Phys. Rev.* 126 (1962) 1977.
- Luque, F.J., Lopez, J.M., Orozco, M. *Theor. Chem. Acc.* 2000, 103, 343.
- Michalska, D. Raint Program, Wroclaw University of Technology, 2003.
- Michalska, D. and Wysokinski, R. *Chem. Phys. Lett.*, 403 (2005) 211-217.
- Mohan, J. *Organic Spectroscopy: Principles and Applications*, second ed., Narosa Publishing House, New Delhi, 2001.
- Nakano, M. Fujita, H. Takahata, M. Yamaguchi, K. Theoretical study on second hyperpolarizabilities of phenyl acetylene dendrimer: toward an understanding of Structure Property relation in NLO responses of fractal antenna dendrimers, *J. Am. Chem. Soc.* 124 (2002) 9648-9655.
- O'Boyle, N.M., Tenderholt, A.L., Langer, K.M.A., library for package-independent computational chemistry algorithms, *J. Comput. Chem.* 2008, 29, 839-845.
- Pople, J.A., Head Gordon, M., & Raghavachari, K. (1987). *Quadratic configuration interaction. A general technique for determining electron correlation energies. Journal of Chemical Physics*, 87, 5968-5975.
- Reed, A.E., Weinhold, F. *J. Chem. Phys.* 1983, 78, 4066-4073.
- Reed, A.E., Weinhold, F. *J. Chem. Phys.* 1985, 83, 1736-1740.
- Reed, A.E., Weinstock, R.B., Weinhold, F. *J. Chem. Phys.* 1985, 83, 735-746.
- Sajan, V., Joe, H., Jayakumar, V.S., Zaleski, J. Structural and electronic contributions to hyperpolarizability in methyl phydroxy benzoate, *J. Mol. Struct.* 785 (2006) 43-53.
- Roeges, N.P.G. *A Guide to the Complete Interpretation of Infrared Spectra of Organic Compounds*, Wiley, New York, 1994.
- Sajan, D., Lynnette Joseph, Vijayan, N., Karabacak, M. *Spectrochim. Acta A* 81 (2011) 85-98.
- Schlegel, H.B. *J. Comput. Chem.* 1982, 3, 214-218.
- Sagdinc, S., Pir, H. *Spectrochim. Acta.* 2009, 73, 181-194.
- Scrocco, E., Tomasi, J. *Adv. Quantum Chem.* 1979, 11, 115.
- Sharma, Y.R. *Elementary Organic Spectroscopy, Principles and Chemical Applications*, S. Chande & Company Ltd., New Delhi, 1994.
- Sharma, A., Khare, R., Kumar, V., Gupta, G.K., Beniwal, V. *Int. J. Pharm. Pharm. Sci.* 2014, 6, 171-175.
- Smith, B. *Infrared Spectral Interpretation. A Systematic Approach*, CRC Press, Washington, D C, 1999.
- Socrates, G. *Infrared Characteristics Frequencies*, Wiley-interscience Publication, New York, 1990.
- Socrates, G. *Infrared Characteristics Group Frequencies*, John Wiley and sons, New York, 1980.
- Sudha, S. Karabacak, M. Kurt, M. Cinar, M. Sundriganesan, N. *Spectrochim. Acta A* 84 (2011) 184-195.
- Vaisalini, N.B., Rao, N.V., Harika, V.B.M.L., Desu, P.K., Nama, S., *Int. J. Pharm. Chem. Res.* 2012, 1, 2278-8700.
- Varsanyi, G. *Vibrational Spectra of Benzene Derivatives*, Academic Press, New York, 1969.
- Zhang, R., Dub, B., Sun, G., Sun, Y., *Spectrochimica Acta A* 75 (2011) 1115-1124.

How to cite this article:

Shakila G *et al* (2018) 'Quantum Computational Analysis of Ethyl 6-(Chloromethyl)-4-(4-Chlorophenyl)-2-Oxo-1,2,3,4-Tetrahydropyrimidine-5-Carboxylate Using Spectral Methods', *International Journal of Current Advanced Research*, 07(2), pp. 10139-10148. DOI: <http://dx.doi.org/10.24327/ijcar.2018.10148.1705>
